Inorganic Chemistry

Article

pubs.acs.org/IC

Long-Range Magnetic Ordering at 5.5 K for Cobalt(II)−Hydroxide Diamond Chains Isolated by 17 Å with α-Phenylcinnamate

Yoshimi Oka,[†,‡] Katsuya Inoue,*[,†,§] Hitoshi Kumagai,[†,∥] and Mohamedally Kurmoo*[,⊥]

[†]Applied Molecular Science, Institute for Molecular Science (IMS), Nishigounaka 38, Myoudaiji, Okazaki 444-8585, Japan

[‡]Frontier Research Core for Life Sciences, University of Toyama, 2630 Sugitani, Toyama 930-0194, Japan

[§]Department of Chemistry, Faculty of Science, Hiroshima University, 1-3-1 Kagamiyama, Higashi Hiroshima, Hiroshima 739-8526, Japan

[∥]Toyota Central R and D Laboratories Inc., 41-1 Yokomichi, Nagakute, Aichi-gun, Aichi, 480-1131, Japan

[⊥]Laboratoire DECOMET, Institut de Chimie de Strasbourg, CNRS-UMR7177, Université de Strasbourg, CS90032, 4 rue Blaise Pascal, Strasbourg 67080, France

Supporting Information

ABSTRACT: $[Co_4(phcina)_6(OH)_2(H_2O)_4]\cdot 2H_2O$ (**1**) (phcina = α-phenylcinnamate), obtained as pink needles by hydrothermal technique, consists of two edge-sharing pairs of octahedral CoO_6 connected by their apexes to form diamond-chains. The magnetic chains are isolated from one another without chemical bond at 17 Å by the nonmagnetic bulky organic ligand. It exhibits hidden canting below the long-range antiferromagnetic (AF) ordering at 5.5 K. A metamagnetic critical field of only 30 Oe at 2 K suffices to overcome the weak through space magnetic interaction between chains and reverse the moments within the chains to give a canted AF reaching only $^1/_4$ of the required moment for all parallel moment alignment. The anisotropy measured on aligned crystals, using dc and ac modes, estimates $g_{\parallel b} = 6.5$ and $g_{\perp b} = 3.25$, thus eliminating an Ising or a Heisenberg magnetic dimensionality while suggesting an easy-plane AF. Weak frequency dependence of the *ac*-susceptibilities below the transition temperature is associated with domain structure in the ordered state, and absence of it well above T_N eliminates single-chain magnetism. It is inferred that the competition between the strong AF coupling between the edge-sharing pairs, which dominates the high temperature susceptibility, and the ferromagnetic coupling within the pairs, results in a canting of the moments within each chain, where the moments are out of the *ac*-plane by an estimated 13°. In zero-field the moments of adjacent chains are antiparallel resulting in a compensated system, i.e., hidden canting.

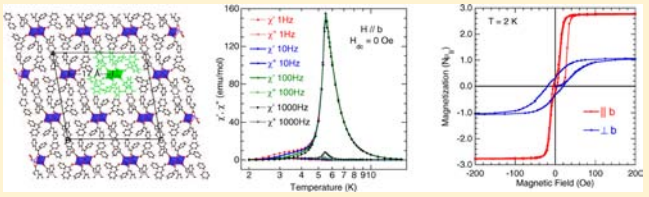

1. INTRODUCTION

The field of magnetism based on metal−organic coordination polymers is a fast moving area of research as one can modify the organic ligands and use transition and/or rare-earth metal ions to form complexes.[1−3] With the wide choice of ligands and metal ions available, a variety of materials have been reported to behave as magnets.[4] These can be crystals of segregated clusters with enough magnetic exchange between them through space leading to long-range magnetic ordering (LRO) at low temperatures.[5,6] However, most are extended lattices, of variable nuclear and magnetic dimensionalities, where the exchange interactions are through bond and the transition temperatures are high and can reach 350 K in rare cases.[7] Several favorite ligands, for example oxalate, cyanide, azide, and small oxoanions (for example: carbonate, squarate, sulfate, etc), have been used regularly with the aim of keeping the distances between the moment carriers short.[8] When the ligands are extended through organic chemistry one aims to retain the moments in layers or chains with M−X−M connections, where X can be halide, N, or O coordinating atoms.[9] Carboxylate containing ligands are of increasing numbers due to the ease of synthesis using the hydrothermal techniques using a normal oven for several days or in minutes by microwave heating.[10] By controlling the concentrations, temperature, and pH one can make different phases that are useful in deriving structure−property relationships. In general, the use of polycarboxylate or pyridine-carboxylate leads to high dimensionality frameworks, where many are magnets.[9] While with monocarboxylate the highest dimensionality is two, but in most cases it is one- or zero-dimension complexes that result. In a previous work we have found that cobalt-cinnamate crystallizes in a 4 × 4 layered structure.[11] By choosing a bulkier ligand α-phenylcinnamate (phcina) to lower the dimensionality we obtained two compounds: one of zero-dimension and the other of one-dimension. We have reported the structure and properties of the zero-dimension compound, $Co_6(phcina)_{10}(OH)_2$ obtained at 170 °C as purple block crystals, which is more condensed and has a $S = 3$ high-spin ground state.[12] Here, we report the structure and properties of the one-dimensional compound,

Received: November 20, 2012
Published: February 5, 2013

   dx.doi.org/10.1021/ic302540h | Inorg. Chem. 2013, 52, 2142−2149

$[Co_4(phcina)_6(OH)_2(H_2O)_4]\cdot 2H_2O$ (**1**), which is obtained at 120 °C as pink needles, and it displays the most exciting observation of long-range antiferromagnetic ordering at 5.5 K when the chains are not chemically connected and exceptionally separated by 17 Å by the bulky phenyl groups of the ligand.

The magnetism of one-dimensional (1D) materials has been of continuing interest by physicists and chemists because it is easier to model and theoretically long-range ordering is not possible.[13,14] However, the wide range of weak interactions between chains in the crystalline state have been responsible for the observation of several classes of one-dimensional magnetic materials, as for example MX_2L_2, AMX_3, etc., where M is a transition metal, X is a halide, A is a alkali ion or an ammonium, and L is a monodentate ligand such as H_2O or pyridine, displaying LRO.[13−15] The physics have been well developed, and the magnetic dimensionality and the effect of local anisotropy are documented.[16] However, more recently we have experienced further developments following the observation of slow relaxation, akin those of single-molecule-magnets,[17] which has been associated to single-chain magnetism (SCM) due to Ising dimensionality which follows the theoretical model of Glauber.[18,19] Consequent to this burst of activity, there are many cases in the literature where distinction between LRO and SCM behavior is not clear-cut.

In this Article we examine the pros and cons for the two cases (LRO and SCM) using a series of experiments to arrive to the conclusion that **1** exhibits long-range magnetic ordering even though the distance between chains are 17 Å, the longest ever in a material to behave as a magnet. We also report the properties of the fully dehydrated compound that behaves as a paramagnet though the interaction between nearest neighbors is quite sizable.

2. EXPERIMENTAL SECTION

Materials and Physical Measurements. All chemicals were obtained from Aldrich, Tokyo Kasei, or Fluka, and used without purification. Infrared spectra were recorded by transmission through KBr pellets containing about 1% of the compound using a JASCO FT-IR spectrometer in the 500−4000 cm^{-1} region. Elemental analyses (C, H, N) were performed on a Yanaco MT-6 CHN analyzer. Thermal analyses (DT-TGA) were performed at a rate of 10 °C/min under Ar using a TA Instruments SDT2960 thermal analyzer. Alternating current and direct current magnetization measurements of **1** were performed on polycrystalline samples using a Quantum Design MPMS-XL SQUID. The ac-field used for the experiments was 5 Oe. The oscillation ac frequencies and the dc applied fields are mentioned for each experiment in the corresponding text and figures.

Preparation of 1. Pink needle crystals of **1** were obtained by the hydrothermal reaction of $Co(NO_3)_2\cdot 6H_2O$ (1.8 g), NaOH (0.25 g), α-phenylcinnamic acid (1.4 g), and water (50 mL) in a Teflon-lined autoclave at 120 °C for 3 days. The resulting crystals were washed with water and acetone and dried in air. The crystals of **1** were manually separated under an optical microscope for further measurements. Yield: 60%. Anal. Calcd for $Co_4O_{20}C_{90}H_{80}$: C 62.94, H 4.70. Found: C 62.72, H 4.91. FT-IR (solid, KBr pellets): ν_{COO} 1630 and 1450 cm^{-1}, ν_{OH} 3600 cm^{-1} (Figure S1).

Crystal Structure Determination. A single crystal was glued on the top of a glass fiber, and diffraction data were collected at room temperature on a Bruker SMART APEX CCD area detector employing graphite monochromated Mo Kα (0.710 73 Å) with ω scan mode. The data were corrected for Lorentz and polarization effects. The structure was solved by direct methods and expanded using Fourier techniques.[20] The non-hydrogen atoms were refined anisotropically and the hydrogen atoms isotropically in theoretical positions. The final cycle of full-matrix least-squares refinement was based on number of observed reflections ($I > 2\sigma(I)$) and n variable parameters and converged (large parameter shift was σ times its esd) with unweighted agreement factors of $R1 = \Sigma||F_o| - |F_c||/\Sigma|F_o|$, $wR2 = [\Sigma w(|F_o| - |F_c|)^2/\Sigma w|F_o|^2]^{1/2}$. No extinction corrections have been applied (Table 1). The supplementary crystallographic data for this paper can be found in the Supporting Information and has been deposited at the Cambridge Crystallography Data Base with the identification number CCDC 217593.

Table 1. Summary of Crystallographic Data of Compound 1

chemical name	Co_4(phenylcinnamate)$_6(OH)_2(H_2O)_4\cdot 2H_2O$
formula	$C_{90}H_{80}Co_4O_{20}$
fw	1717.35
space group	$P2_1/c$ No. 14
a, Å	32.299(2)
b, Å	7.3922(5)
c, Å	34.261(2)
β, deg	100.2180(10)
V, Å^3	8050.4(10)
Z	4
T, K	293(2)
cryst, mm^3	pink needle, 0.5 × 0.04 × 0.03
d g/cm^3	1.417
$F(000)$	3552
μ	0.885
correction	empirical T_{min} = 0.85, T_{max} = 1.00
wavelength, Å	0.710 73
radiation	Mo Kα
R_{int}	0.0622
$\theta_{min} - \theta_{max}$, deg	2.39−28.39
reflns total	18 455
reflns greater than	9466
threshold	$I > 2\sigma(I)$
no. params	1051
no. restraints	0
R (all)	0.1123
R1	0.0563
wR (all)	0.1270
wR2	0.1131
GOF on F^2	0.853
diff density, max, min	1.618, −0.591

3. RESULTS AND DISCUSSION

Structural Description of 1. The key feature of the structure that comes out of the X-ray structure analyses of **1** is the presence of 1D diamond-chains propagating along the crystallographic b-axis separated by the phenyl rings of the bulky organic ligand (Figures 1 and S2) without any chemical connection between them. The b-axis was verified to be along the crystal needle. Each chain is a diagonal strip of a rutile structure resulting in orthogonality between the perpendiculars of the edge-sharing axes of the two pairs. The chains are arranged in a hexagonal closed packed fashion in the ac-plane. There are hardly any π−π interactions and thus the consequent long distance between the chains.

The asymmetric unit consists of four cobalt atoms, two hydroxide, six phcina, and six water molecules belonging to one chain. With $Z = 4$, there are four parallel chains per cell. Within the first pair, the two cobalt centers (Co(1) and Co(3)) exhibit more distorted octahedral geometries (with much longer bond distances of 2.24 and 2.25 Å) than the other pair (Co(2) and Co(4); the typical octahedral Co^{II}(HS), bond distances of 2.03−2.16 Å and O−Co−O bond angles of 81−98°). Co(1)

dx.doi.org/10.1021/ic302540h | Inorg. Chem. 2013, 52, 2142−2149

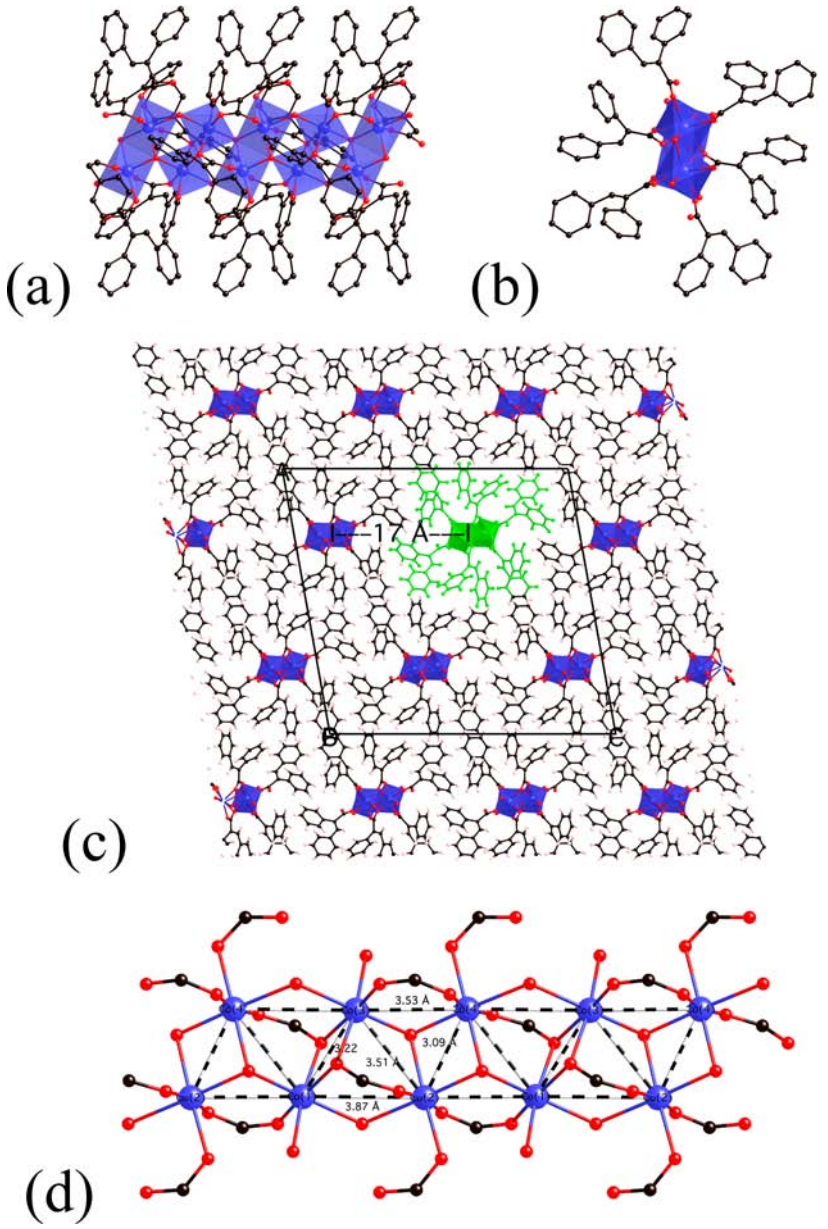

Figure 1. Projection parallel (a) and perpendicular (b) to a chain and the packing of the chains within the unit cell with one highlighted in green (c). The connections and distances between the cobalt atoms within one chain (d).

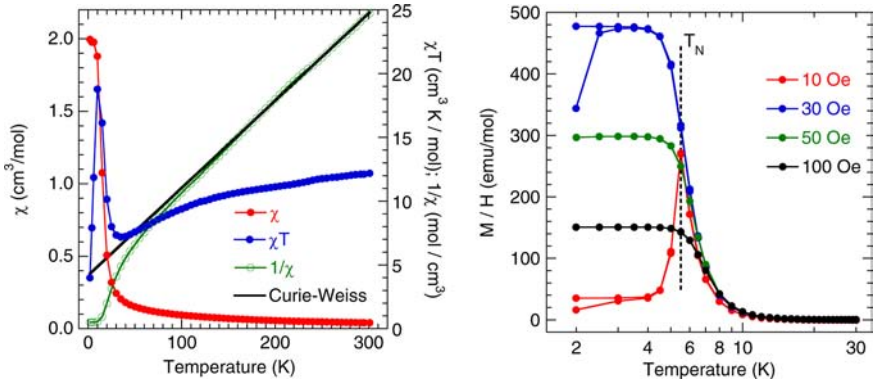

Figure 2. (a) Temperature dependence of the dc-susceptibility, χ (red), the product χT (blue), $1/\chi$ (green), and the Curie–Weiss fit (black line). (b) Temperature dependence of the ZFC and FC dc-magnetization in different applied fields.

dx.doi.org/10.1021/ic302540h | *Inorg. Chem.* 2013, 52, 2142–2149

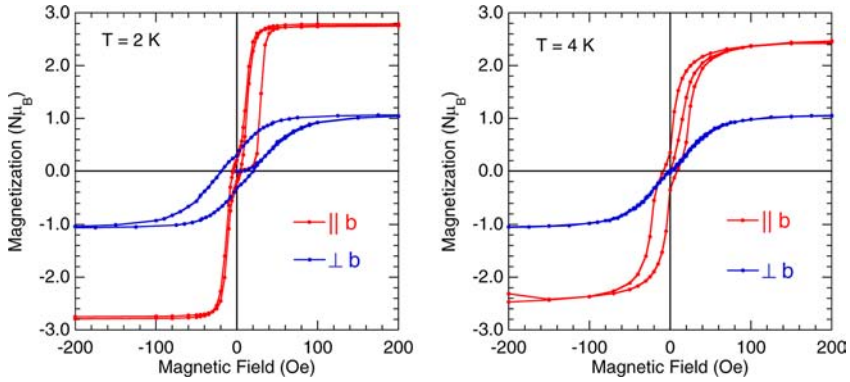

Figure 3. Isothermal magnetization of an array of aligned crystals parallel (red) and perpendicular (blue) to the *b*-axis at 2 K (a) and 4 K (b).

and Co(3) form one edge-sharing pair through the two oxygen atoms of the two μ_3-phcina, and each has another two oxygen atoms from two independent μ_2-phcina (two in bridging mode and one terminal), one bridging water molecule to Co(2) or Co(4), and one terminal water molecule. Co(1)···Co(3) exhibits an intermetallic distance of 3.22 Å and Co(1)−O−Co(3) angles of 96°, which will classify the magnetic interaction between then as ferromagnetic.[9,21,22] Co(2) and Co(4) form the other edge-sharing pair through the two μ_3-OH, and each has three oxygen atoms from three independent phcina (two in bridging mode and one terminal) and one bridging water molecule. Co(2)···Co(4) exhibits the shorter intermetallic distance of 3.09 Å and Co(2)−O−Co(4) angles of 96°, which will also classify the magnetic interaction between then as ferromagnetic. Every other pairwise connection between nearest neighbor cobalt atoms is via two bridges, a Co−O−Co through one oxygen atom of water or hydroxide and the other Co−O−C−O−Co through the carboxylate groups. Both will mediate antiferromagnetic interactions by consideration of the distances and Co−O−Co angles ranging from 117° to 124°.[9,21,22] Thus, one may expect competing effects and frustration although exact triangular motifs are not present. Contrary to the expected single-chain magnetic behavior for chains of the highly anisotropic cobalt(II) separated by such a long distance of 17 Å, long-range magnetic ordering was observed. Consequently, one may envisage these observations as being unique.

Magnetic Properties of 1. *Direct Current Susceptibility.* Temperature dependence of the dc-magnetic susceptibility (χ), the product of susceptibility and temperature (χT), and the inverse susceptibility ($1/\chi$) per Co_4 unit are shown in Figure 2a for a static applied field H_{dc} = 5 kOe using a polycrystalline sample. On decreasing the temperature χT decreases from 12.2 emu K mol^{-1} at 300 K to a minimum of 7.18 emu K mol^{-1} at 35 K, before a rapid increase to a peak near 5 K. Above 100 K the susceptibility obeys the Curie−Weiss law with a Weiss constant (Θ) of −62 K and a Curie constant of 14.5 emu K mol^{-1} per Co_4 unit (that is 3.63 emu K mol^{-1} per Co ion).[23] The effective magnetic moment (μ_{eff}) per Co ion is 5.39 μ_B, which is larger than the expected spin-only value 3.87 μ_B of Co^{II}(HS) due to orbital contribution. For such species, the $^4T_{1g}$ ground triplet splits under the combined action of spin−orbit coupling and crystal-field terms, giving six Kramer's doublets with an effective $S = {}^1/_2$ ground state.[24] The large negative value of Θ indicates the dominant exchange at high temperature to be antiferromagnetic (AF). In contrast, the increase of χT below 35 K suggested the signature of either noncompensation of moment as in a ferrimagnet or ferromagnetic (F) exchange interactions between the near-neighbor Co^{II} ions of the edge-sharing pairs being weaker than the AF ones, principally between pairs, operating at high temperatures. The latter is more probable due to the complete compensation of moments of the two independent pairs of cobalt. The susceptibility in 5 kOe above does not reveal the true ground state characteristics of this material due to metamagnetsim and saturation effects. Thus, the temperature dependences of the magnetic susceptibility for different small applied fields have been recorded in ZFC and FC modes (Figure 2b). Below 10 K, the susceptibility depends strongly on the external field, indicating the presence of large fluctuations of the resulting magnetic moment. First we noticed that in 10 Oe the M/H value goes through a peak at 5.5 K and the FC data divert from the ZFC ones below 4 K. As the field is increased M/H reaches saturation around 30 Oe, and on further increase, it starts to decrease due to saturation effects. Thus, the peak at 5.5 K can be described as the Néel temperature (T_N) of an antiferromagnet, and the critical field of 30 Oe is the metamagnetic transition.[25−28] The nonreversibility between ZFC and FC below 4 K may be due to the presence of a very small canting of the moments (see later).[26,27]

Isothermal Magnetization. To characterize this magnetic transition further, we measured the isothermal magnetization at different temperatures on a powder sample (Figure S3) and on an aligned array of crystals (Figure 3) with field parallel or perpendicular to the needle, that is the crystallographic *b*-axis. The crystals were mounted on a square silicon wafer (4.5 × 4.5 mm^2, Hitachi company) using nonmagnetic silicone grease, and the wafer is fixed in a plastic straw for measurements. No rotation of the crystals was observed after the measurements. This method gives clean, reliable, and reproducible SQUID responses. In contrast, using only one single crystal the signal is too weak. Furthermore, using the Quantum Design rotator the background signal overshadows that from the crystals. The powder sample shows the presence of hysteresis at 2 K and some structures around the zero-field. There is a rapid increase at low field of ca. 20 Oe to reach 2 μ_B and then followed by a linear dependence to reach 2.9 μ_B at 50 kOe. With the field direction set parallel to the *b*-axis (H parallel to the needle axis) at 2 K, the initial magnetization of a virgin sample after ZFC is almost linear up to 30 Oe, and it increases rapidly to 2.7 μ_B at ca. 50 Oe before increasing linearly to 50 kOe. The remanant and saturation magnetizations are 0.2 and 3.2 μ_B/mol, respectively, while the coercive field is 4 Oe, which is within the error of the applied field. On reversing the field the

dx.doi.org/10.1021/ic302540h | *Inorg. Chem.* 2013, 52, 2142−2149

magnetization follows the same track before starting to fall at a field lower than 30 Oe giving a small hysteresis and a smaller one around zero with the return field being symmetric to it.[29] Thus, the initial magnetization is outside the hysteresis loop as has been occasionally observed for some other compounds.[26,27] On increasing the temperature to 4 K, the initial magnetization does not show a critical field but is linear in field while the hysteresis appears more pronounced. When the field is applied perpendicular to the *b*-axis at 2 K, the hysteresis is wide and normal as those of ferrimagnets or ferromagnets, and it almost disappears at 4 K. The observations of a peak in the susceptibility, a critical field for reversing the moments, and presence of hysteresis are clear indications that the magnetic ground state is a long-range ordered antiferromagnet with a weak metamagnetic critical field.[30] From the saturation magnetization values and the shape of the hysteresis, we can infer that **1** is an easy-plane antiferromagnet, with a resultant canted moment from each chain out of the *ac*-plane. The canted moment of one chain is compensated by the opposite alignment of that of the inversion-related chain within the unit cell.[31] Thus, the overall compensation of moments in zero-field is a result of hidden canting.[32] In other words, the through space interaction between nearest neighbor chains is antiferromagnetic.

In the absence of a theoretical treatment for estimating the exchange interactions of chains containing anisotropic moment carriers, we assume the Richard's formula[33] $T_C = CS(S + 1) | JJ'|^{1/2}$ for a Heisenberg one-dimensional systems where J is the average exchange between nearest neighbors within a regular chain and J' the exchange between those of adjacent chains, and use T_C = 5.5 K, C = 3.63 emu K/mol Co, $S_{eff} = {}^1/_2$, and approximate $J \approx 40$ K. Considering the Weiss constant is −62 K, we get $J' \approx 0.03$ K which scales well with the metamagnetic critical field of 30 Oe. Thus, the chains are fairly well isolated from each other magnetically but interact enough to force the moments to order three-dimensionally. As suggested by one reviewer, a useful measure is the ratio k_BT_N/J, which is the relative strength of the order temperature and the intrachain exchange. For the present case the value of 0.14 is low but is comparable to other $S = {}^1/_2$ chains which display LRO.[34] It is important to note that more elaborate theory will be required for anisotropic ions with orbital contribution, and furthermore, the presence of both ferromagnetic and antiferromagnetic exchange interactions within each chain in the present case will have to be considered, though the complexity will make it even more difficult.

Magnetic Model. In the absence of exchange interaction between chains, the existence of LRO for such isolated magnetic chains would be quite intriguing given that theoretically there should not be 3D ordering. The low critical field of 30 Oe is a measure of the energy scale of the interaction between chains, which is very weak due to the absence of any chemical bonds and the long distance between neighboring chains, and therefore, its presence confirms independently the LRO state. Taking the nearest neighbor interactions within the chain in consideration as we have mentioned earlier that there are two ferromagnetically coupled pairs that are antiferromagnetically coupled between them, we may expect a frustrated system. Given that the values (3.2 μ_B ||b and 1.0 μ_B ⊥b) of the moment attained in a high field of 50 kOe are far lower than the 10 μ_B expected for four Co(II) moments being parallel, we infer that the moments of each pair may be canted away from the *b*-axis. The canting within the chains will present a linear dependence of the magnetization at the high field ends, which is the case along both directions of applied field. Using the results of the *ac*-susceptibility anisotropy of $g_{||b}$:$g_{\perp b}$ is 2, and assuming the two $g_\perp$ valuess to be equal and the sum of g's to be 13 for Co(II), we can estimate $g_{||b}$ = 6.5 and $g_{\perp b}$ = 3.25. If we take the saturation value for $H_{||b}$ of 3 μ_B and the expected saturation to be ngS which is $4 \times 6.5 \times {}^1/_2 = 13$, the canting angle is estimated as $\sin^{-1}(3/13) = 13.34°$ from the *ac*-plane. It is quite possible that the ferromagnetic couplings between pairs (Co1−Co3 and Co2−Co4) tend to force the moments to be Ising, i.e., along the *b*-axis, while the antiferromagnetic interactions have a preference for XY in the *ac*-plane. Since the magnitude of the AF coupling is larger than that of the F coupling, the moments are driven to give an easy-plane antiferromagnetic ground state. Therefore, the proposed model in Figure 4 consists of eight magnetic sublattices (8 cobalt pairs) consisting of the four independent cobalt atoms per chain and their inversion symmetry related counterparts in the other chains of the unit cell. The verification of such a model would require a full analysis of the neutron diffraction data above and below the magnetic ordering transition temperature. This experiment is currently hampered by the need to have a fully deuterated sample of large quantities (10 g). This is not presently feasible in the present work.

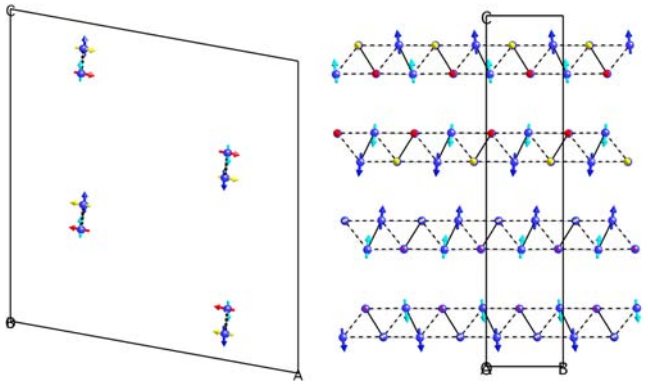

Figure 4. Proposed zero-field magnetic structure viewed along *b* and *a*. The solid black bonds represent ferromagnetic exchanges and the dashed bonds the antiferromagnetic exchanges pathways.

Alternating Current Susceptibilities. In order to evaluate the balance between the long-range ordered state and that of a single-chain magnetic state, we explored the temperature dependence of the ac-susceptibilities as a function of the frequency of the oscillating field and the bias applied dc-field (Figures 5, 6, S4, and S5). Early measurements were performed on a polycrystalline sample with random orientation and, subsequently, on the array of aligned single crystals with field parallel and perpendicular to the *b*-axis. On the powder sample for the real component, we observe a frequency-independent sharp peak at 5.5 K and a shoulder at lower temperatures that disappears gradually with increasing frequency. For the imaginary component, there is a peak aligning with the shoulder of the real component, and it develops into two peaks as the frequency is increased and accompanied by a shift to higher temperatures. This behavior resembles that of the ferrimagnet $K_2Co^{II}_3(OH)_2(SO_4)_3(H_2O)_2$ where the shift in the peak of χ'' was associated to the temperature dependence of the domain shape which in principle should be the same for the present compound.[35] It is to be noted that there were some

dx.doi.org/10.1021/ic302540h | *Inorg. Chem.* 2013, 52, 2142−2149

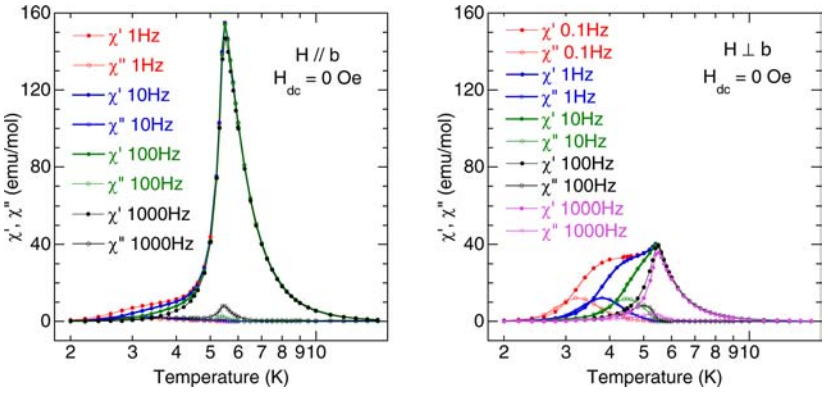

Figure 5. Temperature dependence of the ac-susceptibilities at different frequencies in zero bias dc-field for field parallel (a) and perpendicular to the *b*-axis (b).

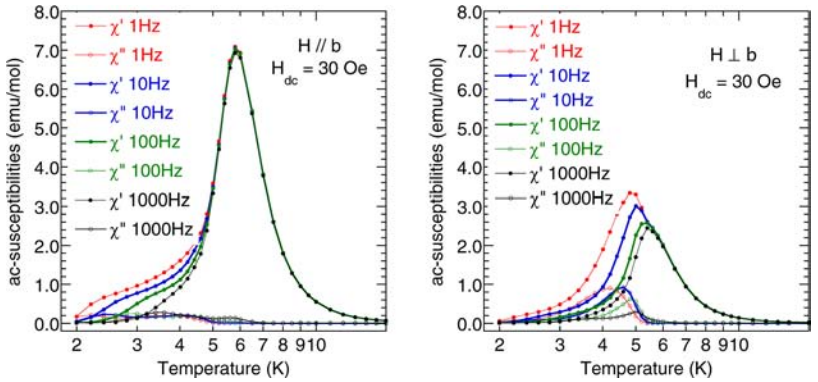

Figure 6. Temperature dependence of the ac-susceptibilities at different frequencies in 30 Oe bias dc-field for field parallel (a) and perpendicular (b) to the *b*-axis.

nonzero values of χ'' for temperature between 5.5 and 6.5 K. As a function of applied field to 100 Oe, a peak is observed at 30 Oe at 2 K, and this peak is over 200 times in intensity at 4 K while it is centered at 20 Oe. On increasing the temperature the peak once again becomes weak and disappears by 5 K. This is consistent with doing a mutual inductance experiment and also suggests a normal phase diagram for a metamagnet.

When the ac-field is parallel to the *b*-axis, the real component of the ac-susceptibility is sharp and strong in contrast to the imaginary part that is weak. The peak is at 5.5 K and it is frequency independent but the shoulder centered at ca. 4 K is frequency dependent. The imaginary part becomes nonzero at 5.5 K for 1 Hz, and there is a weak broad peak at the shoulder. On increasing the frequency there is a peak appearing at 5.5 K that is frequency independent, and the broad maximum with the shoulder shifted toward higher temperature. It is also to be noted that for higher frequencies (>10 Hz) there are nonzero values for the imaginary part above 5.5 K. When the *ac*-field is perpendicular to the *b*-axis, the intensity of the peak in the real part at 5.5 K is comparable to that of the shoulder but is four times less intense, and they display the same frequency behavior as above. In contrast the imaginary part displays only one peak which peaked with the shoulder and shifted to higher temperatures on increasing the frequency. The observation of the ac-susceptibilities for orientated crystals clearly explains the complexities of those of the powder sample. The temperature dependence of the real part for the two orientations suggests that the axis of high magnetization is the *b*-axis (the direction of the canting of the moments) as is the isothermal magnetization, and second, the values are consistent with those expected for an anisotropic antiferromagnet. From this observation we can conclude that $\chi_{\parallel}:\chi_{\perp}$ is 4; thus, $g_{\parallel}:g_{\perp}$ is 2. These values are too small for one to consider this diamond chain as being Ising, thus eliminating the possibility of observing Glauber's dynamics as expected for Ising single-chain magnetism. However, there are some very unusual dynamics that are associated with domains within this canted antiferromagnet, although one may consider the domain to be more prominent within the chains rather than encompassing various unit cells in the *ac*-plane. The presence of an imaginary component of the *ac*-susceptibilities extending just above the transition temperature of 5.5 K is a clear indication of the presence of a domain structure within each chain, before the material orders antiferromagnetically, as a consequence of the exponential increase of the coherent length of the superparamagnetism as temperature approaches the transition temperature. The frequency dependence for SCM monitoring the blocking temperature usually extends over a wider temperature range.[17,18] Understanding the domain structure above and below the transition temperature of this material is beyond the scope of this paper and requires theoretical treatment that is not presently available.

Long-Range Order versus Single-Molecule-Magnetism. As we have inferred earlier that magnetic domains are present in this compound, resulting in the observation of hysteresis, and that the domains are principally within the chains, it is therefore worthwhile to evaluate the relaxation processes in order to distinguish between LRO and SCM as this is a hot topic, and there are several schools with very wide views. First to clarify the nature of the relaxation process (Figure S6), the peak temperature of χ'' can be scaled with the parameter $\Phi = (\Delta T/$

dx.doi.org/10.1021/ic302540h | *Inorg. Chem.* 2013, 52, 2142−2149

$T)/\Delta(\log \nu)$ giving values of 0.13 and 0.12 for $\parallel$ and $\perp$ orientations, respectively, which are much larger than that for a typical spin glass (where Φ is around 0.01), but more typical for superparamagnetism.[36] Thus, the frequency dependence may be associated with domain wall motion. The process of such relaxation is usually associated with overcoming the energy barriers at an absolute temperature T with a characteristic relaxation time, τ. Subsequently, the thermal variation of τ is described by the Arrhenius law

$$\tau = \tau_0 \exp[E_a/k_B T]$$

where τ_0 is a coefficient and E_a is the energy barrier separating the different states of the magnetic moments. If $\tau = 1/\omega$ where $T = T_B$ is supposed, the equation can be rewritten as

$$\frac{1}{\omega} = \frac{1}{\omega_0}\exp[E_a/k_B T]$$

$$\ln \omega = \ln \omega_0 - (E_a/k_B T)\frac{1}{T_B}$$

where $\omega = 2\pi\nu$, ν is the driving frequency of the ac-field, and T_B is the blocking temperature at which χ'' has the maximum value. ω_0 and E_a were determined from a plot of $\ln(2\pi\nu)$ versus $1/T_B$. The best parameters obtained are $\tau_0 = 1.9 \times 10^{-11}$ s and $E_a/k_B = 64$ K for parallel direction, and $\tau_0 = 1.8 \times 10^{-11}$ s and $E_a/k_B = 89$ K for perpendicular direction. These values of energy barriers indicate that domain wall mobility of parallel direction is larger than that of perpendicular direction. Furthermore, the values of τ_0 and E_a for perpendicular direction mean that the relaxation time of the magnetization associated with domain wall displacement is on the order of 12 years at 2 K and 0.08 s at 4 K. Thus, hysteresis loop of perpendicular orientation was observed at 2 K and not observed at 4 K.

With a bias dc field of $H = 30$ Oe ($>H_C$) applied in the same direction as the ac-field, the frequency dependence of the ac-susceptibilities has been observed for randomly oriented sample, for parallel to b-axis (Figure 6a) and for perpendicular to b-axis (Figure 6b). The peak temperature of χ'' can be related to the parameter $\Phi = (\Delta T/T)/\Delta(\log \nu) = 0.15$ and 0.06 for $\perp b$ and $\perp b$ orientations, respectively. The best fitting parameters obtained using Arrhenius law are $\tau_0 = 3.1 \times 10^{-7}$ s and $E_a/k_B = 27$ K for parallel direction, and $\tau_0 = 1.7 \times 10^{-19}$ s and $E_a/k_B = 176$ K for perpendicular direction. The processes of slow magnetic relaxation cannot be represented by a linear term of magnetic field below 4 K. The analysis of this process is difficult, and the results require advances in theory that is presently lacking. However, the indication is that **1** is not behaving as Ising, and the absence of large frequency dependence to higher temperatures and the presence of the weak interchain interaction justified by the metamagnetic transition are all against the conditions for the observation of single chain magnetism behavior. Furthermore, the g-value anisotropy also eliminates its description as Heisenberg, leaving XY as the only possibility.

Thermal and Magnetic Property after Dehydration. The thermogravimetric analyses under argon show that complete dehydration of the compound takes place between 105 and 115 °C followed by the decomposition into cobalt oxide above 380 °C (Figure S7). The dehydration is accompanied by a weight loss of 5.5% compared to 5.5% calculated for six water molecules. The loss of water is also observed in the infrared spectrum of a sample annealed at 125 °C for 3 h and leaving the band for ν_{OH} at 3600 and 3630 cm^{-1} for the hydrated and dehydrated sample, respectively, and the antisymmetric and symmetric ν_{COO} bands at 1630 and 1450 cm^{-1} for both samples (Figure S1). These observations suggest the structure may be preserved after dehydration but with the geometries of the cobalt atoms changed to tetrahedral for Co1 and Co3 and pentacoordination for Co2 and Co4. This is expected to change the anisotropy of the material considerably. The dc-magnetic susceptibilities of a collection of crystals of **1** annealed at 400 K for 3 h in a flow of helium in the SQUID magnetometer, that is, $[Co_4(phcina)_6(OH)_2]$, were measured. The product of the susceptibility and temperature and the inverse of the susceptibility per Co_4 unit are presented in Supporting Information (Figure S8), for a static applied field $H_{DC} = 5$ kOe. The χT value of 9.77 emu K mol^{-1} at 300 K decreases gradually to 2 K. The Curie–Weiss fit above 100 K exhibits a Weiss constant of −68.3 K and a Curie constant of 10.7 emu K mol^{-1} per Co_4 unit (2.68 emu K mol^{-1} per Co ion). The effective magnetic moment (μ_{eff}) per Co unit is 4.63 μ_B. The low value compared to **1** is as expected due to the change in geometries of the cobalt coordination. There is no indication of long-range magnetic ordering down to 2 K (Figure S9). The isothermal magnetization at 2 K only reaches 2.5 μ_B per Co_4 at 50 kOe, that is, a quarter of the expected for a pure paramagnetic compound, thus reflecting the large antiferromagnetic coupling between the cobalt ions.

4. CONCLUSION

Long-range magnetic ordering has been demonstrated for a hydrothermally synthesized complex, $[Co^{II}_4(phcina)_6(OH)_2(H_2O)_4]\cdot 2H_2O$, which consists of cobalt-hydroxide diamond-chain of edge-sharing pairs connected via their apexes and separated from each other by 17 Å by the bulky phenylcinnamate (phcina). The magneto-structural study, using both ac- and dc-magnetization as a function of temperature, field, and frequency, reveals very complicated magnetic behaviors not encountered previously that are discussed in terms of chains having XY anisotropic with $S_{eff} = {}^1/_2$, $g_{\parallel b} = 6.5$, and $g_{\perp b} = 3.25$. The moments are inferred to have a canting angle of 13.34° from the XY (ac) plane due to competing ferromagnetic interaction within pairs and antiferromagnetic interactions between them. The moments of the neighboring chains are canted in the opposite direction to lead to compensated antiferromagnetism below 5.5 K in zero-field. The ground state is therefore a hidden-canted antiferromagnet. The existence of domains was suggested by the frequency dependence of the ac-susceptibility and the presence of hysteresis. The long distance between the antiferromagnetically coupled chains and the absence of chemical links allow a very weak metamagnetic critical field of 30 Oe to reverse the moments to give a resultant of 3 μ_B (a quarter of that expected for parallel alignment) along the b-axis. The results show a clear contrast to those expected for a single-chain magnet that is required to be Ising and the frequency dependence of the ac-susceptibilities extending to higher temperatures from the blocking one at low frequency. Dehydration of the compound changes the coordination geometries of the cobalt atoms, and thus their magnetic anisotropies, and consequently, this results in the absence of long-range ordering. The present results confirm that interactions through space occupied by electron density in molecular magnetic materials can be important for long-range magnetic ordering of moments at fairly long distances.

dx.doi.org/10.1021/ic302540h | Inorg. Chem. 2013, 52, 2142–2149

■ ASSOCIATED CONTENT

Supporting Information

X-ray crystallographic information file in CIF format. DT-TGA traces and infrared spectra. Susceptibility measured on cooling in different magnetic fields. This material is available free of charge via the Internet at http://pubs.acs.org.

■ AUTHOR INFORMATION

Corresponding Author

*E-mail: kxi@hirosima-u.ac.jp (K.I.); kurmoo@unistra.fr (M.K.).

Notes

The authors declare no competing financial interest.

■ ACKNOWLEDGMENTS

This work was supported by a Grant-in-Aid for Scientific Research (A) (222 45023) from the ministry of Education, Culture, Sport, Science and Technology (MEXT), Japan, and the CNRS (France).

■ REFERENCES

(1) *Metal-Organic and Organic Molecular Magnets*; Day, P., Underhill, A. E., Eds.; Philosophical Transactions of the Royal Society 357; Royal Society: London, 1999.

(2) Carlin, R. L. *Magneto-Chemistry*; Springer-Verlag: Berlin, 1986.

(3) (a) *Magnetism: A Supramolecular Function*; Kahn, O., Ed.; Kluwer Academic Publishers: Berlin, 1996. (b) *Molecular Magnetism, New Magnetic Materials*; Itoh; K., Kinoshita, M., Eds.; Gordon Breach-Kodansha: Tokyo, 2000.

(4) See the Proceedings of the International Conference on Molecule-Based Magnets: *Polyhedron*, **2007**, **2009**, **2011**.

(5) (a) Kinoshita, M. *Jpn. J. Appl. Phys.* **1994**, *33*, 5718. (b) Blundell, S. J.; Pratt, F. L. *J. Phys.: Condens. Matter* **2004**, *16*, R771.

(6) Carlin, R. L.; De Jongh, L. *J. Chem. Rev.* **1986**, *86*, 659.

(7) Verdaguer, M.; Bleuzen, A.; Marvaud, V.; Vaissermann, J.; Seuleiman, M.; Desplanches, C.; Scuiller, A.; Train, C.; Garde, R.; Gelly, G.; Lomenech, C.; Rosenman, I.; Veillet, P.; Cartier, C.; Villain, F. *Coord. Chem. Rev.* **1999**, *190*−*192*, 1023.

(8) (a) Ohba, M.; Okawa, H. *Coord. Chem. Rev.* **2000**, *198*, 313. (b) Batten, S. R.; Murray, K. S. *Coord. Chem. Rev.* **2003**, *246*, 103. (c) Ribas, J.; Escuer, A.; Monfort, M.; Vicente, R.; Cortés, R.; Lezama, L.; Rojo, T. *Coord. Chem. Rev.* **1999**, *193*−*195*, 1027.

(9) Kurmoo, M. *Chem. Soc. Rev.* **2009**, *38*, 1353.

(10) (a) Chen, Q.; Zeng, M.-H.; Wei, L.-Q.; Kurmoo, M. *Chem. Mater.* **2010**, *22*, 4328. (b) Zhou, Y.-L.; Zeng, M.-H.; Wei, L.-Q.; Li, B.-W.; Kurmoo, M. *Chem. Mater.* **2010**, *22*, 4295.

(11) Kumagai, H.; Oka, Y.; Inoue, K.; Kurmoo, M. *J. Chem. Soc., Dalton Trans.* **2002**, 3442.

(12) Kumagai, H.; Oka, Y.; Kawata, S.; Ohba, M.; Inoue, K.; Kurmoo, M.; Okawa, H. *Polyhedron* **2003**, *22*, 1917.

(13) De Jongh, L. J.; Miedema, A. R. *Adv. Phys.* **1974**, *23*, 1.

(14) Steiner, M.; Villain, J. *Adv. Phys.* **1976**, *25*, 87.

(15) Harrison, A. *J. Phys: Condens. Matter* **2004**, *16*, S553.

(16) *Magnetic Properties of Layered Transition Metal Compounds*; De Jongh, L. J., Ed.; Kluwer Academic Publishers: Dordrecht, The Netherlands, 1990.

(17) Gatteschi, D.; Sessoli, R.; Villain, J. *Molecular Nanomagnets*, Oxford University Press: Oxford, 2006.

(18) (a) Caneschi, A.; Gatteschi, D.; Lalioti, N.; Sangregorio, C.; Sessoli, R.; Venturi, G.; Vindigni, A.; Rettori, A.; Pini, M. G.; Novak, M. A. *Angew. Chem., Int. Ed.* **2001**, *40*, 1760. (b) Clérac, R.; Miyasaka, H.; Yamashita, M.; Coulon, C. *J. Am. Chem. Soc.* **2002**, *124*, 12837. (c) Coulon, C.; Clérac, R.; Lecren, L.; Wernsdorfer, W.; Miyasaka, H. *Phys. Rev. B* **2004**, *69*, 132408. (d) Coulon, C.; Miyasaka, H.; Clérac, R. *Struct. Bonding (Berlin)* **2006**, *122*, 163.

(19) Glauber, R. J. *J. Math. Phys.* **1963**, *4*, 294.

(20) Sheldrick, G. M. *Acta Crystallogr.* **2008**, *A64*, 112.

(21) Goodenough, J. B. *Magnetism and the Chemical Bond*; John Wiley and Sons: New York, 1963.

(22) (a) Kanamori, J. *J. Phys. Chem. Solids* **1959**, *10*, 87. (b) Kanamori, J. In *Magnetism*; Rado, G. T., Suhl, H., Eds.; Academic Press: New York, 1963; Vol. *I*, Chapter. 4, p 127.

(23) Blundell, S. J. *Magnetism in Condensed Matter*; Oxford University Press: Oxford, 2001.

(24) Schieber, M. M. *Selected Topics in Solid State Physics Experimental Magnetochemistry*; Wohlfarth, E. P., Ed.; North-Holland: Amsterdam, 1967; Vol. *VIII*.

(25) Rujiwatra, A.; Kepert, C. J.; Claridge, J. B.; Rosseinsky, M. J.; Kumagai, H.; Kurmoo, M. *J. Am. Chem. Soc* **2001**, *123*, 10584.

(26) Kumagai, H.; Kepert, C. J.; Kurmoo, M. *Inorg. Chem.* **2002**, *41*, 3410.

(27) Kurmoo, M.; Kumagai, H.; Green, M. A.; Lovett, B. W.; Blundell, S. J.; Ardavan, A.; Singleton, J. *J. Solid State Chem.* **2001**, *159*, 343.

(28) Marvilliers, A.; Parsons, S.; Riviere, E.; Audiere, J.-P.; Kurmoo, M.; Mallah, T. *Eur. J. Inorg. Chem.* **2001**, *5*, 1287.

(29) Chikazumi, S. *Physics of Ferromagnetism*, 2nd ed.; Clarendon Press: Oxford, 1997.

(30) Weng, D.-F.; Wang, Z.-M.; Gao, S. *Chem. Soc. Rev.* **2011**, *40*, 3157.

(31) Ben Salah, M.; Vilminot, S.; André, G.; Bourée-Vigneron, F.; Richard-Plouet, M.; Mhiri, T.; Kurmoo, M. *Chem. Mater.* **2005**, *17*, 2612.

(32) (a) Carlin, R. L.; Van-Duyneveldt, A. J. *Magnetic Properties of Transition Metal Compounds*; Springer-Verlag: New York, 1977. (b) Carlin, R. L. *Magnetochemistry*; Springer-Verlag: Berlin, 1986. (c) Herweijer, A.; de Jonge, W. J. M.; Botterman, A. C.; Bongaarts, A. L. M.; Cowen, J. A. *Phys. Rev. B* **1972**, *5*, 4618. (d) Kopinga, K.; van Vlimmeren, Q. A. G.; Bongaarts, A. L. M.; de Jonge, W. J. M. *Physica B +C* **1977**, *86*−*88*, 671. (e) Basten, J. A.; van Vlimmeren, Q. A. G.; de Jonge, W. J. M. *Phys. Rev. B* **1978**, *18*, 2179. (f) Engelfriet, D. W.; Groeneveld, W. L.; Groenendijk, H. A.; Smit, J. J.; Nap, G. M. *Z. Naturforsch.* **1980**, *35A*, 115. (g) Carlin, R. L.; Joung, K. O.; van der Bilt, A.; del Adel, H.; O'Connor, C. J.; Sinn, E. *J. Chem. Phys.* **1981**, *75*, 431.

(33) Richards, P. M. *Phys. Rev.* **1974**, *810*, 4687.

(34) Blundell, S. J.; Lancaster, T.; Pratt, F. L.; Baker, P. J.; Brooks, M. L.; Baines, C.; Manson, J. L.; Landee, C. P. *J. Phys. Chem. Solids* **2007**, *68*, 2039.

(35) Vilminot, S.; Baker, P. J.; Blundell, S. J.; Sugano, T.; Andre, G.; Kurmoo, M. *Chem. Mater.* **2010**, *22*, 4090−4095.

(36) Mydosh, J. A. *Spin Glasses: An Experimental Introduction*; Taylor & Francis: London, 1993.